

Supporting Information

OFF/ON galvanic replacement reaction for preparing divergent AuAg nano-hollow as a SERS-visualized drug delivery system in targeted photodynamic therapy.

Chih-Chia Huang‡, Pei-Hua Lin‡ and Chien-Wei Lee*

Department of Photoics, National Cheng Kung University, Tainan 70101, Taiwan

***Corresponding authors:** Prof. Chih-Chia Huang

E-mail: c2huang@mail.ncku.edu.tw; huang.chihchia@gmail.com

‡ These authors contributed equally

Experimental

Materials. Hydrogen tetrachloroaurate(III) trihydrate ($\text{HAuCl}_4 \cdot 3\text{H}_2\text{O}$), 99.9% (Alfa Aesar), poly(styrene-alt-maleic acid) sodium salt solution (PSMA) (Aldrich), methylene blue (MB) (Alfa Aesar), sodium chloride (NaCl) (Fisher chemical), silver nitrate (AgNO_3) (Fisher chemical), dimethyl sulfoxide (DMSO) (Fisher chemical), terephthalic acid (TA), 98% (Alfa Aesar), Nitric acid (HNO_3) (Fisher chemical), hydrogen peroxide solution (H_2O_2) (SIGMA-ALDRICH), polyvinylpyrrolidone (PVP, M.W. = 55,000) (Aldrich), ethylene glycol (EG) (Fisher chemical), copper(II) nitrate 2.5-hydrate, (J. T. Baker), chlorophyll iron sodium (Haining Fengming Chlorophyll Co., Ltd. China), and HS-PEG₃₅₀₀-NH₂ (JenKem Technology) were purchased for use without further purification.

Synthesis of Ag nanoparticles. AgNO_3 (0.025 g) and polyvinylpyrrolidone (PVP) (0.10 g) were dissolved in 10 mL of ethylene glycol with vigorous stirring. The solution was heated at 160 °C for 1.5 h, yielding an Ag colloidal solution with a green-yellow color.^{1,2} After cooling to room temperature, the resulting solution was stocked as the template solution for the subsequent hollowing reaction.

Synthesis of Ag nanocubes. Six mL of ethylene glycol was heated in an oil bath at 150 °C to remove H_2O . Polyvinylpyrrolidone (PVP) (0.02 g) was added in the pre-treated ethylene glycol (6 mL) with vigorous stirring. 0.28 mL of NaSH (3 mM) was subsequently added. 2 mL-ethylene glycol included AgNO_3 solution (76 mg) was poured into the above mixture solution and reacted at 150 °C for 0.5 h. After cooling in an ice bath, the resulting solution was collected by centrifuging and washed with acetone for 1 time. The product was re-dispersed in ethylene glycol and was stocked as the template solution for the subsequent hollowing reaction.

Synthesis of Ag nanoplates. Ag nanoprism was provided by Prof. Cheng-Liang Huang at National Chiayi University (Taiwan). Sample was prepared according to the previous synthesis method.³

Synthesis of Cu₂O nanoparticles. Cu(NO₃)₂·2.5H₂O (0.0278 g) and polyvinylpyrrolidone (PVP) (0.10 g, MW: 55,000) were dissolved in 10 mL of ethylene glycol with vigorous stirring. The solution was heated at 160 °C for 2 h, yielding a Cu₂O colloidal solution with a light yellow color. After cooling to room temperature, the resulting solution was stocked as the template solution for the subsequent hollowing reaction.

Synthesis of 3-D AuAg nano-hollows. A volume of 0.125 mL of Ag colloidal solution (14.7 mM) was added to 2.5 mL of PSMA solution (240 mg/10 mL) with vigorous magnetic stirring. The resulting aqueous suspension was further reacted with 4 mL of a 0.04 mM-HAuCl₄·3H₂O aqueous solution using a dropwise addition process. Then, 0.2 mL of HNO₃ solution (0-0.22 M) was immediately added to the above reaction mixture for another 3.5 min until the color became stable. To remove the excess ions, polymers, and AgCl solid byproduct, the 3-D AuAg nano-hollows were collected using centrifugation at 10000 rpm for 10 min, were then washed with a saturated NaCl solution, and were rinsed with deionized water more than three times.

Synthesis of smooth surface structured AuAg nano-hollows. This sample preparation was similar to the synthesis of the 3-D AuAg nano-hollows except for the addition of the PSMA polymer solution. Typical reactions can be found in the literature.^{1,2} The SPR absorption band of smooth surface structured AuAg nano-hollows did not change after addition of the HNO₃ solution.

Raman measurement of AuAg nano-hollows containing target objects. For all of the SERS measurements, a 5 μL aliquot of the AuAg nano-hollow sample solution (~ 500 ppm) was directly mixed with 5 μL of the targeting molecule (e.g., MG, MB, and sodium iron chlorophyllin). These solutions were carefully transferred onto the respective Si substrate using a micropipette and were subjected to micro-Raman spectroscopy using a 785 nm laser (10.6 mW) and an MRS-iHR320 modular Raman system. The Raman enhancement factor of the AuAg nano-hollow-containing substrate was determined using the following equation:

$$EF = (I_{SERS} / I_{free\ substrate}) \times (N_{free\ substance\ concentration} / N_{AuAg\ nano-hollows-containing\ substance\ concentration})$$

where I_{SERS} and $I_{free\ MB}$ indicate the vibration scattering intensities in the SERS and normal Raman spectra, respectively. I_{SERS} and $I_{free\ MB}$ were calculated for the strongest peak of the targeting substrates. $N_{free\ substance\ concentration}$ and $N_{AuAg\ nano-hollows-containing\ substance\ concentration}$ represent the concentration of substance molecules on the surface of a Si wafer. In the EF estimation, we assumed that the substance molecules in the liquid drop were homogeneously distributed on the Si wafer and exposed to the incident laser beam.

Preparation of 3-D AuAg@MB nano-hollows and folic acid-conjugated 3-D AuAg@MB nano-hollows. For the preparation of the folic acid-conjugated 3-D AuAg nano-hollows, 200 μ L of 3-D AuAg nano-hollows solution (250 ppm_[metal]) was pre-modified with HS-PEG-NH₂ polymer (200 μ L at 2 mg/mL) with at 4 °C for 24 h, allowing that the SH groups at the PEG polymer the chemically bind to the surface of 3-D AuAg nano-hollows, and their primary amine groups would be completely exposed at the surface. After purifying with a centrifugation and re-dispersion process, the as-prepared 3-D AuAg@PEG-NH₂ nano-hollow solution was reacted with 0.85 mL of activated folic acid solution including ~ 1.5 μ M folic acid, ~ 7 mg/mL N-(3-Dimethylaminopropyl)-N'-ethylcarbodiimide hydrochloride (EDC), and ~ 7 mg/mL N-Hydroxysuccinimide (NHS). After 30 min, the activated AuAg nano-hollow was centrifuged at 10,000 rpm for 20 min at 4 °C to remove excess folic acid and EDC/NHS, and the particles were resuspended in 1 ml of PBS.

Hereafter, methylene blue was loaded into 3-D AuAg nano-hollows (120 μ L, 0.1 mM) and folic acid-conjugated 3-D AuAg nano-hollows by mixing AuAg nano-hollow (120 μ L, 0.1 mM) with methylene blue (1.5 μ L, 5 mM) to prepare 3-D AuAg@MB nano-hollows and folic acid-conjugated 3-D AuAg@MB nano-hollows, respectively. These mixtures were placed at 4 °C. Over 12 hrs of interaction time room temperature for 12 h, the first

supernatant was detected by a UV-Visible spectrometer to calculate the loading of MB by centrifugation (10 000 rpm for 10 min). The MB-absorbed AuAg samples were purified by washing twice with Milli-Q water and dispersed in 100 μ L PBS buffer solution.

SERS microscopic imaging. HeLa cervical cancer cells were cultured in Dulbecco's modification of Eagle's medium with 10% fetal bovine serum at 37 °C under 5% of CO₂ in air before SERS spectral analysis. HeLa cells were pre-cultured in an 8-well Lab-Tek™ chamber slide™ (20000 cells per well) for 1 day. After incubation, the original medium was removed, and 0.2 mL of folic acid-absorbed 3-D AuAg@MB nano-hollows (25 ppm_[metal]) was added for co-culture with the cells. After 0.25 h and 6 h of incubation, the supernatant solution was carefully discarded, and then the particle-treated cells on the slide were washed with PBS. Subsequently, the cell-containing chamber slide™ was transferred to a custom-built micro-Raman spectroscopy instrument by an integration of Jobin-Yvon LabRAM high resolution Raman spectrometer (Horiba iHR 320) and Olympus BX3 microscopes to obtain individual Raman signals at different positions in the cellular images. A 40 × objective lens was used to collect point to point signals with a computer-controlled x, y-stage in 4.0 μ m increments using a Raman microscope. Each data point was obtained during a 1 s acquisition. All spectral controls, manipulations, and data analysis were performed using LabRAM systems.

Photothermal therapy (PTT) and photodynamic therapy (PDT) experiments. HeLa cells were seeded into 96-well cell-culture plates at 8000 cells/well and incubated for 24 h at 37 °C under 5 % CO₂. After incubating the cells with experiment groups, the standard MTT [3-(4, 5)-dimethylthiaziazolo-2-yl-2,5-diphenyltetrazolium bromide] metabolic activity assay was carried out to determine the cell viabilities relative to the control untreated cells. We investigated the reactive oxygen species (ROS) level in the 660 LED-irradiated cancer cells through ROS staining with 2, 7-

dichlorofluorescein diacetate (DCF-DA) dye by using confocal laser scanning microscopy (Olympus FluoView 1000 confocal laser scanning microscope, Japan).⁵

12.5 ppm_[metal] of 3-D AuAg@MB nano-hollows and folic acid-conjugated 3-D AuAg@MB nano-hollows were dispersed in the culture media. Next, 100 μ L of the particle containing medium was added to each well. We replaced the particle containing medium with a fresh one after the particles were incubated with the HeLa cells for 0.25 h and 2 h. PDT (applied by a 660 nm LED at 10 mW/cm² for 4 min) and PTT (applied by a 808 nm laser at 380 mW/cm² for 3 min) treatments were carried out. For the PDT \rightarrow PTT the combination therapy were conducted by firstly exposed to the 660-nm light for 4 min and subsequently irradiated with the 808-nm laser for 3 min. For PTT \rightarrow PDT group, the particle-treated cells were firstly irradiated with the 808 nm-laser for 3 min, and then exposed to the 660-nm light for 4 min. After another 1 day of incubation, the cell viability in all experiment groups was measured by an MTT assay. Cell viability was reported as a percentage calculated as a ratio between the treated groups and the control group (without particles and light treatment).

References

1. Y. G. Sum, B. T. Mayers, Y. Xia, *Nano Lett.*, 2002, **2**, 481.
2. X. Xia, Y. Wang, A. Ruditskiy, Y. Xia, *Adv. Mater.*, 2013, **25**, 6313.
3. B. H. Lee, M. S. Hsu, Y. C. Hsu, C. W. Lo, C. L. Huang, *J. Phys. Chem. C*, 2010, **114**, 6222.
4. J. Planeta, P. Karásek, M. Roth, *J. Phys. Chem. C*, 2009, **113**, 9520.
5. Yu, C. H. Hsu, C. C. Huang, P. Y. Chang, *ACS Appl. Mater. Interfaces.*, 2015, **7**, 432.
6. G. B. Deacon, R. J. Phillips, *Coord. Chem. Rev.*, 1980, 33, 227—250.
7. G. B. Deacon, F. Huber, R. J. Phillips, *Inorg. Chim. Acta*, 1985, 104, 41—45.
8. F. Huang, D. Chen, X. L. Zhang, R. A. Caruso, Y. B. Cheng, *Adv. Funct. Mater.*, 2010, **20**, 1301.
9. K. Chaudhari, P. L. Xavier, T. Pradeep, *ACS Nano*, 2011, **5**, 8816.
10. M. J. Kim, H. J. Na, K. C. Lee, E. A. Yoo, M. Lee, *J. Mater. Chem*, 2003, **13**, 1789.
11. C. Sangregorio, M. Galeotti, U. Bardi, P. Baglioni, *Langmuir*, 1996, **12**, 5800.
12. S. Senapati, A. Ahmad, M. I. Khan, M. Sastry, R. Kumar, *Small*, 2005, **1**, 517.

Table S1. The corresponding SPR peak of the PVP/PSMA-protected Ag in the H_{AuCl}₄ solution with the different HNO₃ concentrations.

HNO ₃ concentrations (M)	SPR peak position (nm)
0	428
0.02	436 and 620
0.06	437and 636
0.11	524
0.16	670
0.22	694
0.66	694

The preparation of PVP-protected Ag colloid (14.71 mM) in ethylene glycol was performed according to previously reported methods.^{1,2} The size of the solid Ag nanoparticles was determined to be 62 ± 4.4 nm. These Ag colloids exhibited a strong SPR band at 421 nm (Figure S1a). A HR-TEM image showed a polycrystalline structure (2-3 nm) for single Ag nanoparticles (Figure S1b).

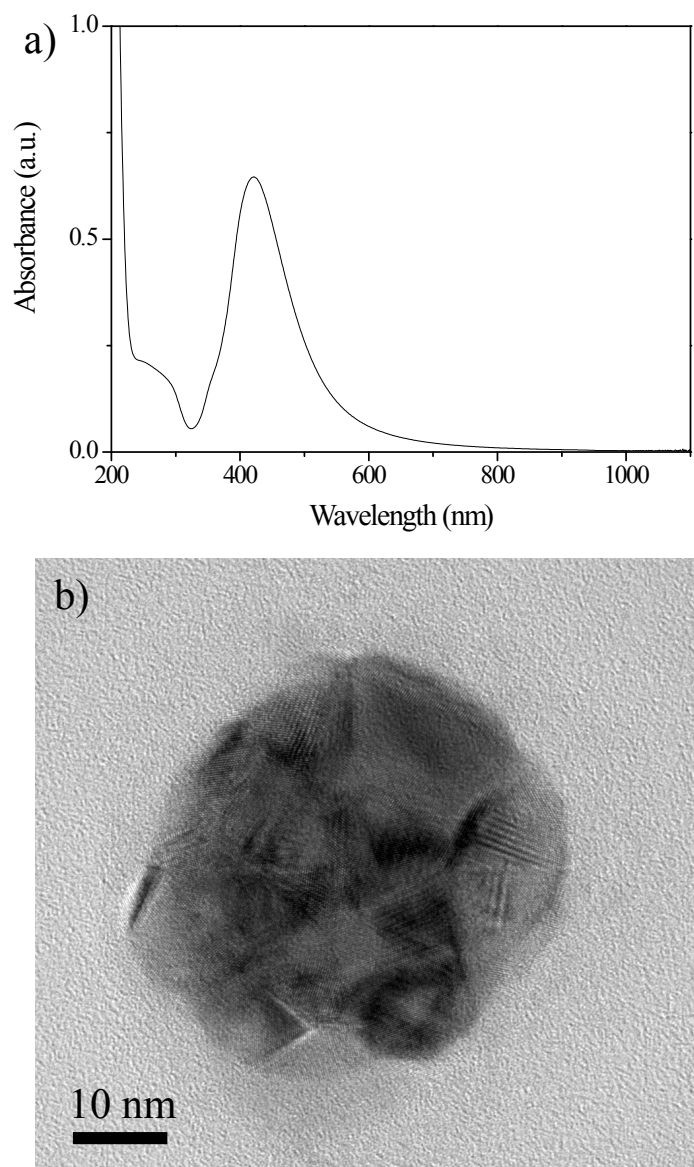


Figure S1. a) UV-visible spectrum and b) HR-TEM image of the as-prepared Ag nanoparticle solution.

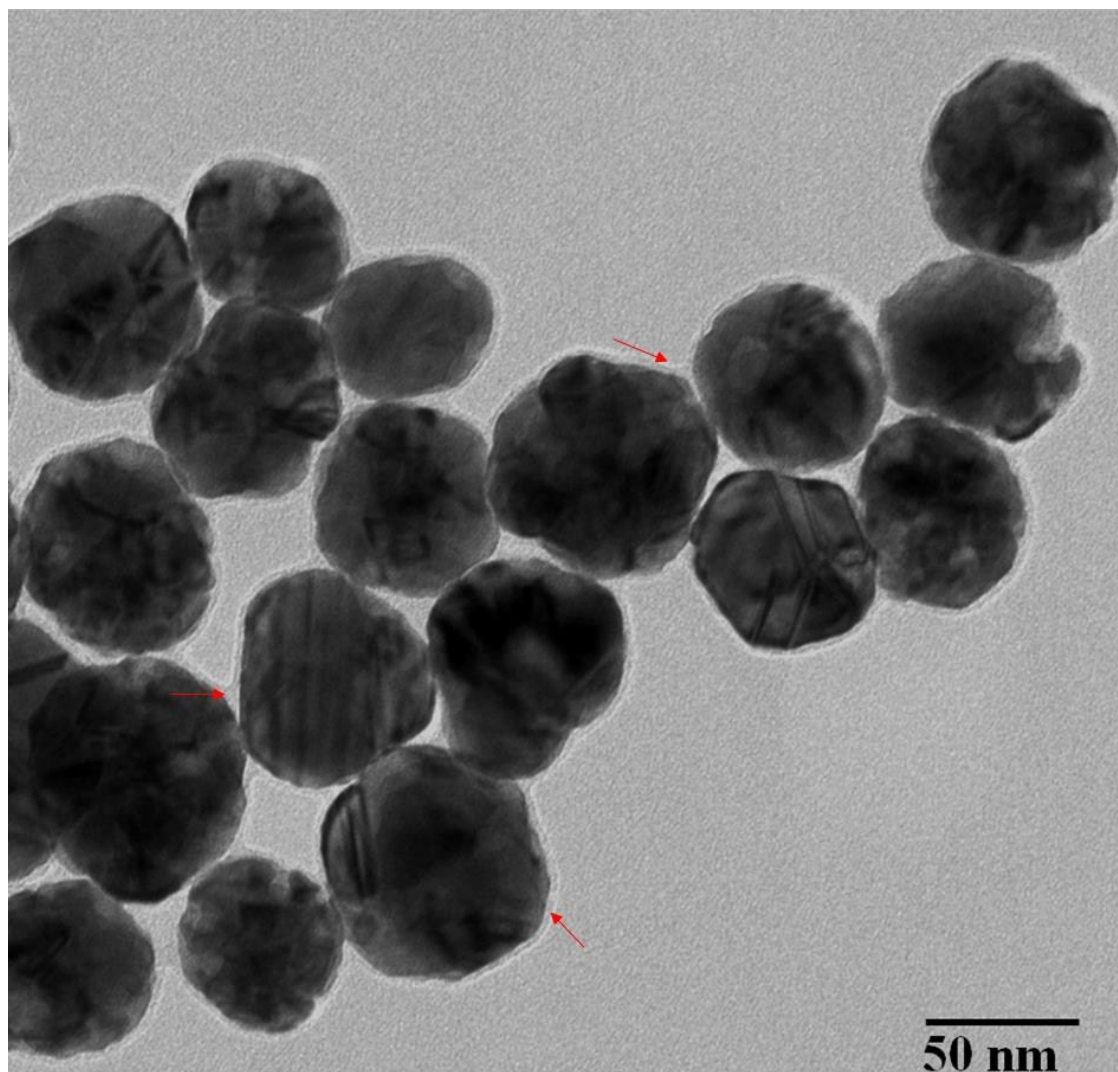


Figure S2. High-magnification TEM image of PSMA/PVP-protected Ag nanoparticles.

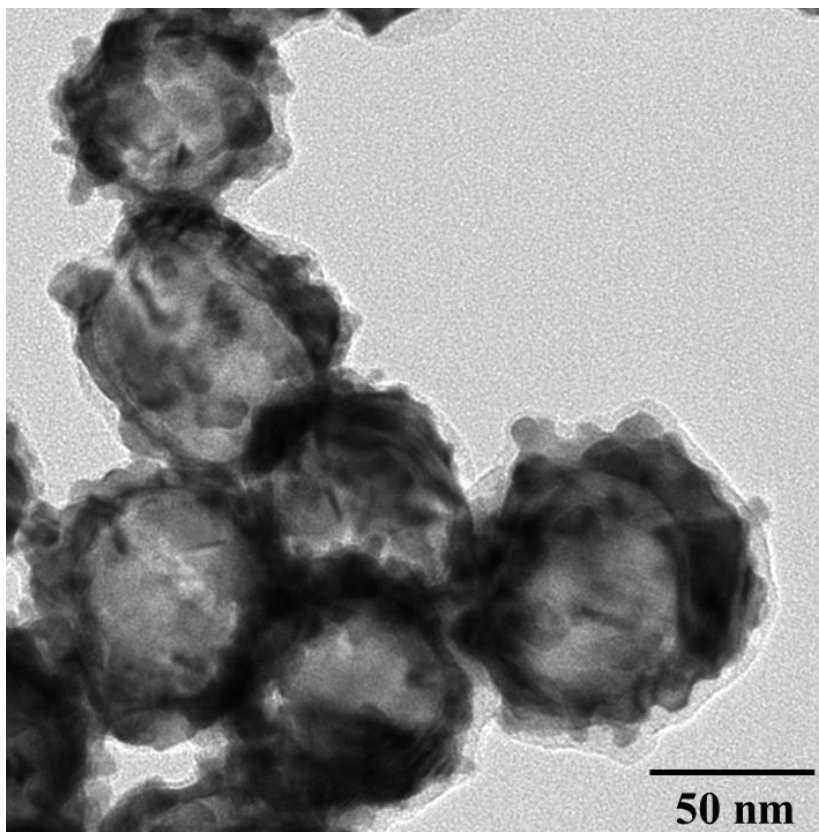


Figure S3. High magnification TEM image (120 kV) of the 3-D AuAg nano-hollows.

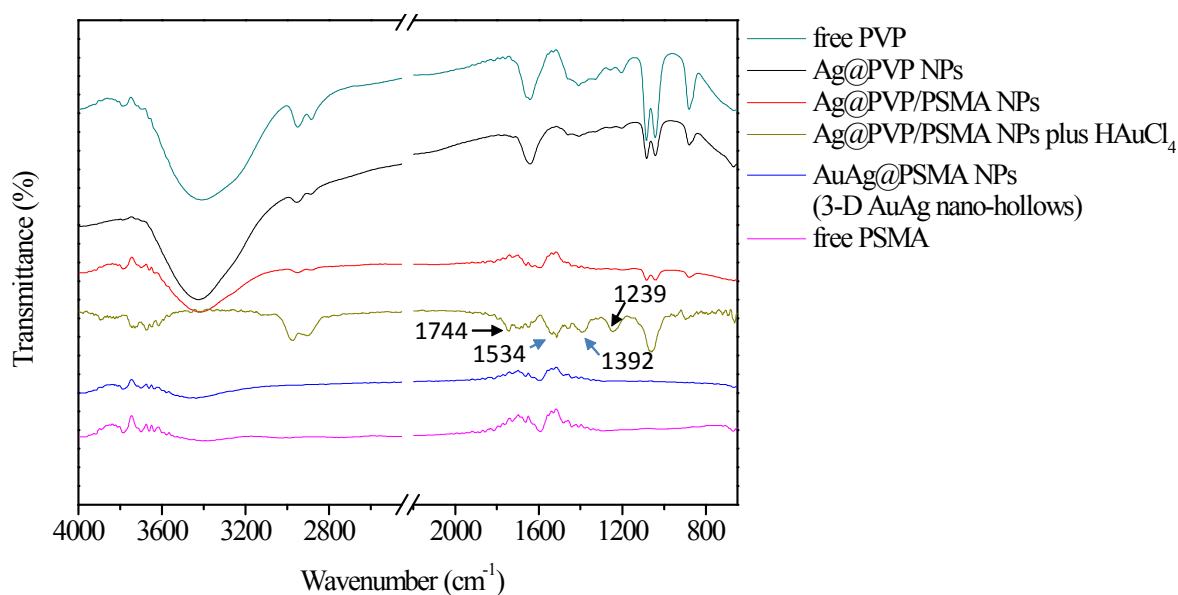


Figure S4. a) FT-IR spectra of PVP-protected Ag nanoparticles, PVP/PSMA-protected Ag nanoparticles, 3-D AuAg nano-hollows, free PVP polymer, and free PSMA polymers. Noted that an additional IR peak at $\sim 1596\text{ cm}^{-1}$ (red-color arrow) of C=C stretching by PSMA polymer was obtained for PSMA-immobilized Ag@PVP NPs. In the analysis of the precipitate sample purified from the Ag@PVP/PSMA plus HAuCl₄ solution, the blue-color arrows at 1534 cm^{-1} and 1392 cm^{-1} were due to the $\nu_{\text{as}}(\text{COO}^-)$ and $\nu_{\text{a}}(\text{COO}^-)$ groups, respectively, which bonded to Au ions, The Δ value between $\nu_{\text{as}}(\text{COO}^-)$ and $\nu_{\text{a}}(\text{COO}^-)$ groups is about is 142 cm^{-1} , suggesting the complicated forms of chelating and/or bridging coordination.^{6,7} Two main peaks by black-color arrows at 1744 cm^{-1} and 1239 cm^{-1} was assigned to the carbonyl stretching of non-dissociated COOH group and C–O stretching of COOH, respectively.

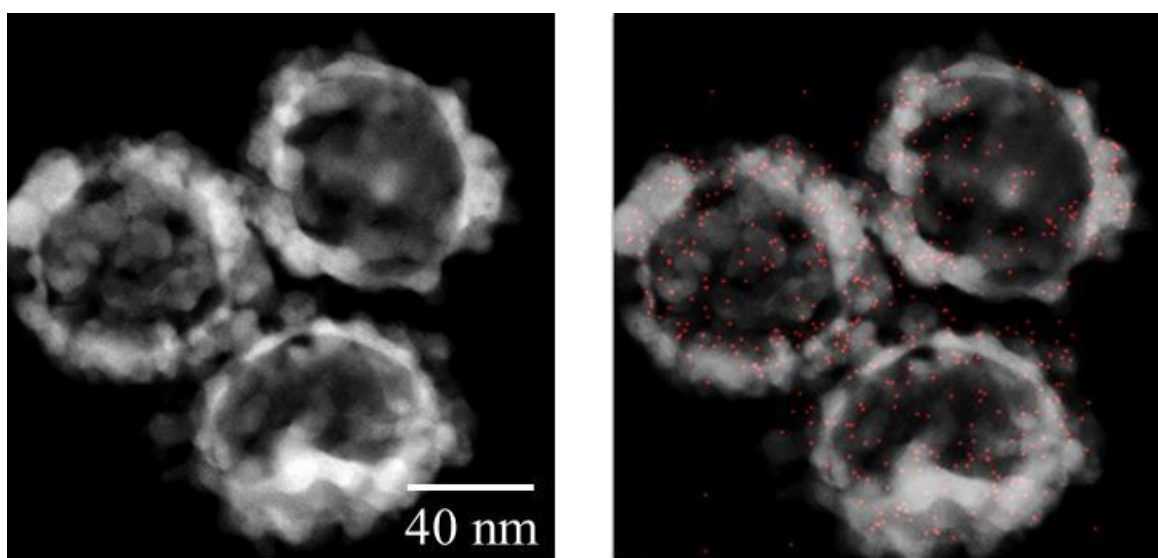


Figure S5. STEM-HAADF image (left) and EDS elemental map of Au atoms overlapped with a STEM-HAADF image (right) of the 3-D AuAg nano-hollows.

Furthermore, we performed additional SEM and TEM imaging (Figure S6) to study the concentration effect of HNO_3 on the formation of 3-D AuAg nano-hollows. Using a 0.02 M HNO_3 solution, a single pore inside the Ag nanoparticle was generated. The number of Ag NPs with a single pore structure increased as the HNO_3 concentration increased to 0.05 M. Using HNO_3 volumes ranging from 0.02 mM to 0.11 M, the size of the pore in the interior of the particle increased, while the surface of Ag NPs appeared as a relatively flat structure. The formation of a rough surface on the resulting nanoparticle was found after the addition of 0.16 M HNO_3 . In addition, we conducted UV-visible spectrometry to monitor this acid-induced Ag structure hollowing process. A trend toward red-shifting of the SPR bands was observed during the formation of 3-D AuAg nano-hollows with increasing HNO_3 concentrations (Figure S7a and Table S1). The maximum absorption intensity rarely decreased, the peak became broader, and all NIR wavelengths showed strong absorbance. When more than 0.22 M of HNO_3 was used, the optical curve of the resulting 3-D AuAg nano-hollow was rarely changed (Figure S7a) due to the consistent structure morphology (Figure S8).

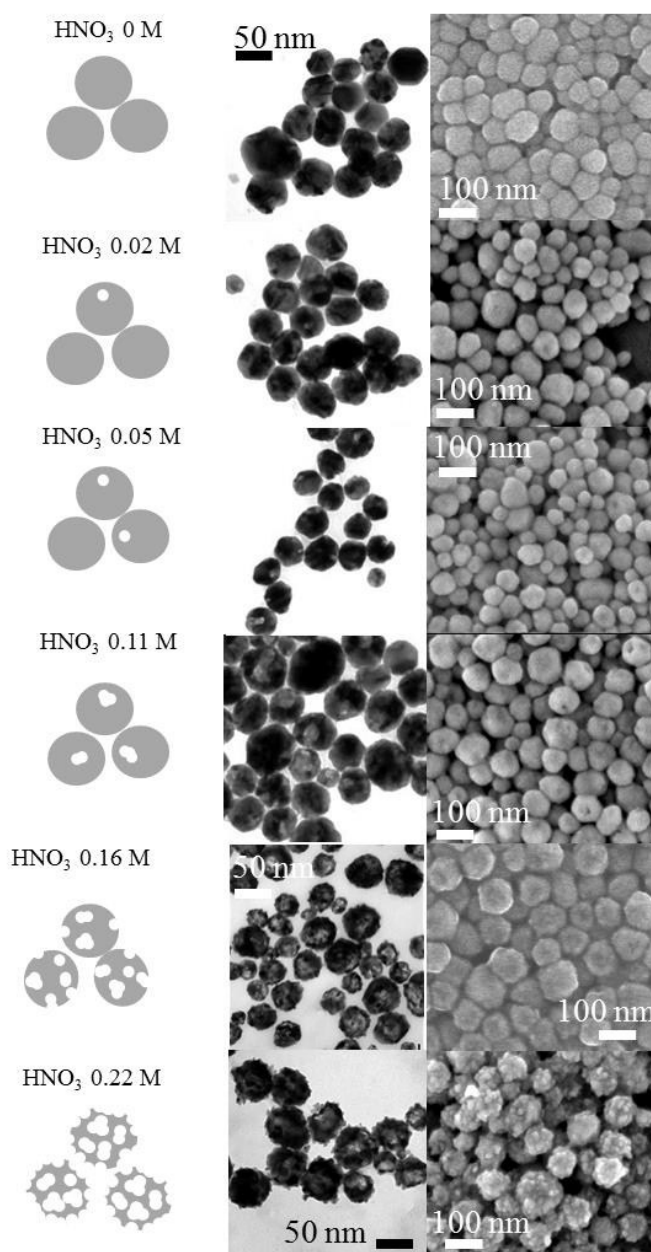


Figure S6. TEM and SEM images of the PSMA/PVP-protected Ag nanoparticles after 4 mL of HAuCl_4 solution was reacted with different concentrations of HNO_3 solution.

The 3-D AuAg nano-hollow exhibited a strong excitation coefficient at NIR wavelengths (i.e., 785 nm, 808 nm, and 1064 nm) compared to AuAg nano-hollows with smooth surfaces with the same nano-Ag particle number and HAuCl_4 precursor concentration. Presumptively, porous hollow nanoparticles have lower light scattering ability and can absorb many photons.⁸ We employed an 808 nm laser (580 mW/cm^2) to excite the plasmonic 3-D AuAg nano-hollow (80 ppn) with a type K thermocouple (Figure S7d). A value of $\Delta T = \sim 40 \text{ }^\circ\text{C}$ was determined after 6 min. When the excitation wavelength was changed from 808 nm to 256 nm, the 3-D AuAg nano-hollows heated the solution to greater than $45 \text{ }^\circ\text{C}$ ($\Delta T = \sim 20 \text{ }^\circ\text{C}$). However, a solution containing smooth surface AuAg nano-hollows showed great excitation wavelength-dependent consequences with values of ΔT of $26 \text{ }^\circ\text{C}$ at 808 nm and $11.2 \text{ }^\circ\text{C}$ at 1064 nm.

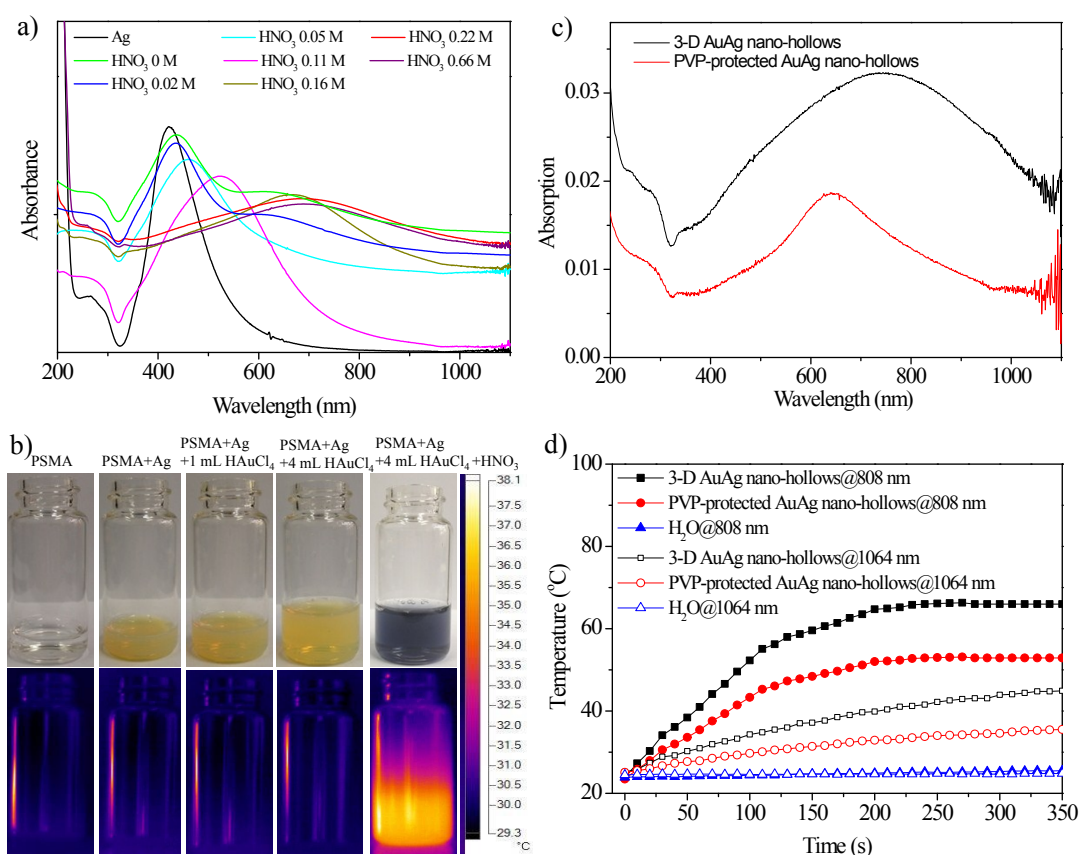


Figure S7. a) UV-visible spectra of the pH-induced reaction of the PSMA/PVP-protected Ag nanoparticles in the HAuCl_4 solution with the different HNO_3 concentrations. b) The bright-field (top) and thermal imaging camera images were used to monitor the in situ reaction of the PSMA/PVP-protected Ag colloidal solution with the HAuCl_4 and HNO_3 solutions. An 808 nm laser was employed at 1.27 W/cm^2 . c) UV-visible measurement of the PVP-protected AuAg nano-hollows and 3-D AuAg nano-hollows. d) Temperature dependence of laser (808 nm and 1064 nm)-irradiated H_2O , PVP-protected AuAg nano-hollows and 3-D AuAg nano-hollows as a function of irradiation time at a power density of 580 mW/cm^2 .

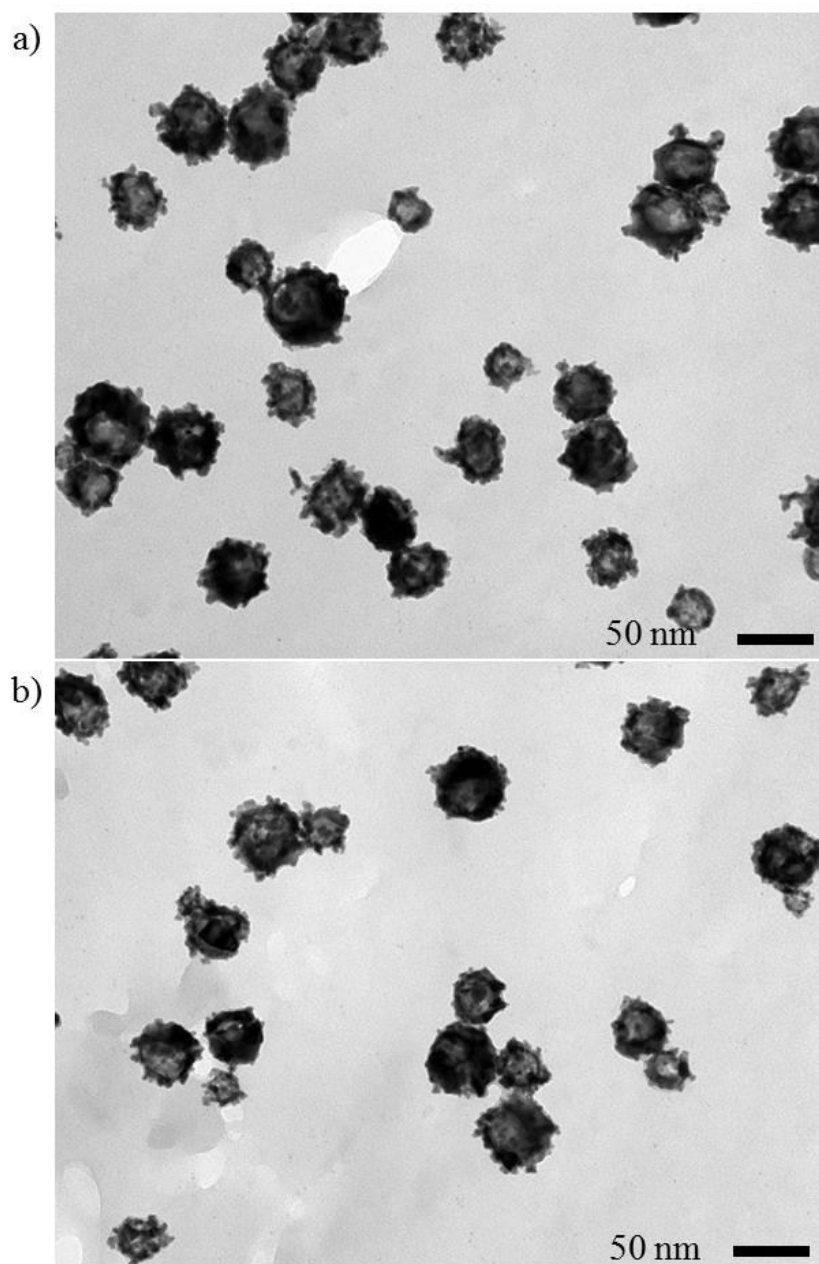


Figure S8. TEM images of the PSMA/PVP-protected Ag nanoparticles after 4 mL of HAuCl_4 solution was reacted with a) 0.44 M and a) 0.66 M HNO_4 solution (0.2 mL).

After adding HAuCl_4 solution to the Ag@PVP/PSMA solution, two broadening binding energy bands, $4f_{7/2}$ and $4f_{5/2}$, were detected for the HAuCl_4 -treated Ag NPs (Figure S9a). Interestingly, the $4f_{5/2}$ peak showed signals at three individual regions, 88.1 eV, 89.2 eV, and 91.3 eV, which could be due to the existence of Au(0), Au(I), and Au(III) species, respectively.^{9,10} At least 50% of Au was estimated to be in the ionic state at the surface of Ag NPs before the reaction with HNO_3 solution. These ions might complex with the PSMA polymer. With half of the solution consisting of 0.11 M HNO_3 , the portions of the Au(I) and Au(III) ions were significantly decreased in the overall Au composites at the particle surface, providing strong evidence for the release of the Au ions from PSAM-Au motifs. Accordingly, the ratio of Ag to Au was decreased through an H^+ -triggered confinement galvanic replacement reaction accompanied by a slight down-shifting of the corresponding $3d_{5/2}$ peak from 368.3 eV to 368.2 eV (Figure S9b). In addition, the peak $4f_{7/2}$ of the metallic Au state at 84.4 eV was shifted to 84.5 eV. Previous investigations have demonstrated that the shifting in the binding energy of metallic Au at the 4f peak and metallic Ag at the 3d peak are indicative of the formation of an AuAg alloy.^{11,12}

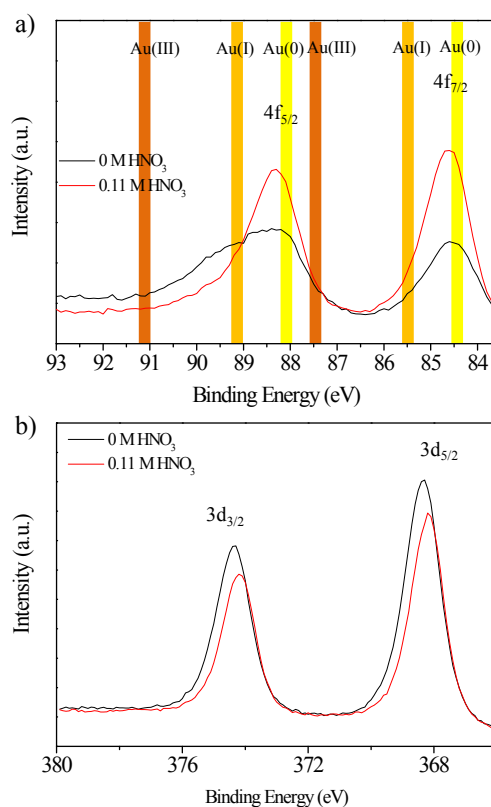


Figure S9. XPS spectra of PSMA/PVP-protected Ag nanoparticles reacted with HAuCl_4 solution after adding HNO_3 solutions: a) Au 4f and b) Ag 4f. The relationship between the atomic ratio of $\text{Au}/(\text{Au}+\text{Ag})$ and the concentration of added HNO_3 solution.

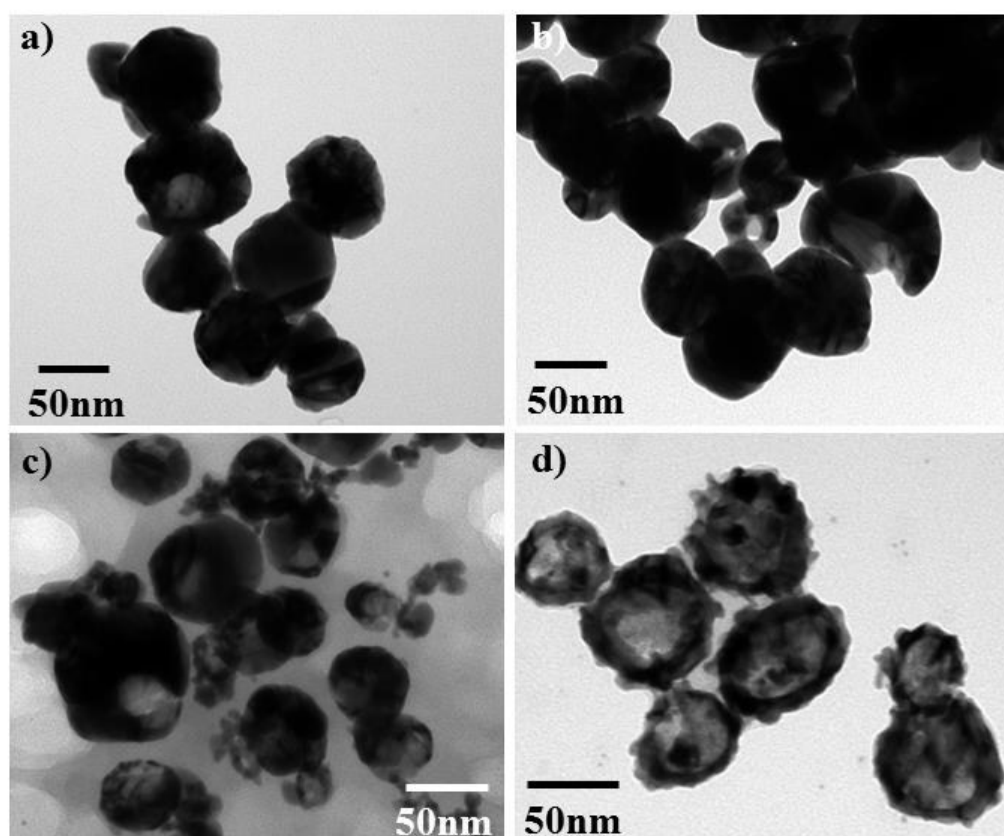


Figure S10. TEM images of the PSMA/PVP-protected Ag nanoparticles after 4 mL of HAuCl_4 solution reacted with a) NaOH, b) NaCl, c) FeCl_2 , and d) HCl solutions.

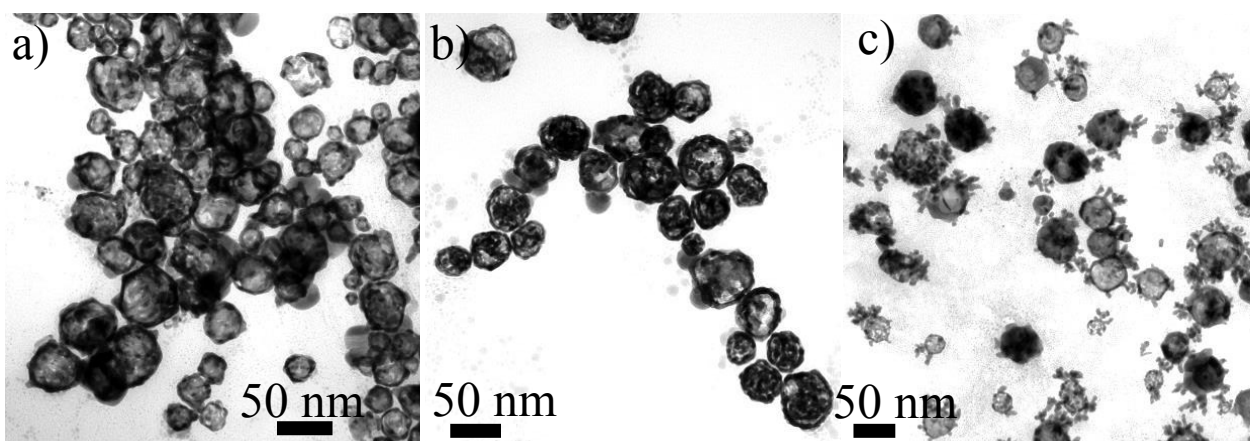


Figure S11. TEM images of the a) PEG/PVP-, b) PAH/PVP-, and c) PAA/PVP-protected Ag nanoparticles after 4 mL of HAuCl_4 solution was reacted with 0.22 M HNO_4 solution (0.2 mL).

We explored this PSMA-resisted and H^+ -triggered confinement galvanic replacement reaction with the aim of preparing other 3-D and porous hollow structures consisting of Au-based NPs. TEM images determined that the resulting nanoproducs consisted of 3-D and cube-like AuAg nano-hollows (Figure S12a), porous hollow and plate-shaped AuAg nanoplates (Figure S12b), and porous hollow Au/Cu₂O nanopolyhedrons (Figure S12c) that were fabricated using Ag nanocubes (0.67 mM), Ag nanoplates (0.35 mM), and Cu₂O nanopolyhedrons (0.67 mM) (Figure S13), respectively, as the starting materials. The inset in Figure S12a shows a HR-TEM image of nodular surface structure at an AuAg nanobox. Similarly, the colloidal colors of the Ag nanocube (green-yellow) and Ag nanoplate solution (blue) remained after the reaction with the HAuCl₄ solution; then, the colloidal colors were changed by adding the HNO₃ solution (Figure S14). UV-visible measurement (Figure S12d) determined the appearance of dramatic absorption bands toward NIR wavelengths for the 3-D AuAg nanocubes and porous AuAg nanoplates. The Au grown on the surface of Cu₂O nanopolyhedrons exhibited a plasmonic behavior after the oxidation of the Cu₂O portions of the interior of the nanopolyhedrons (Figure S15).

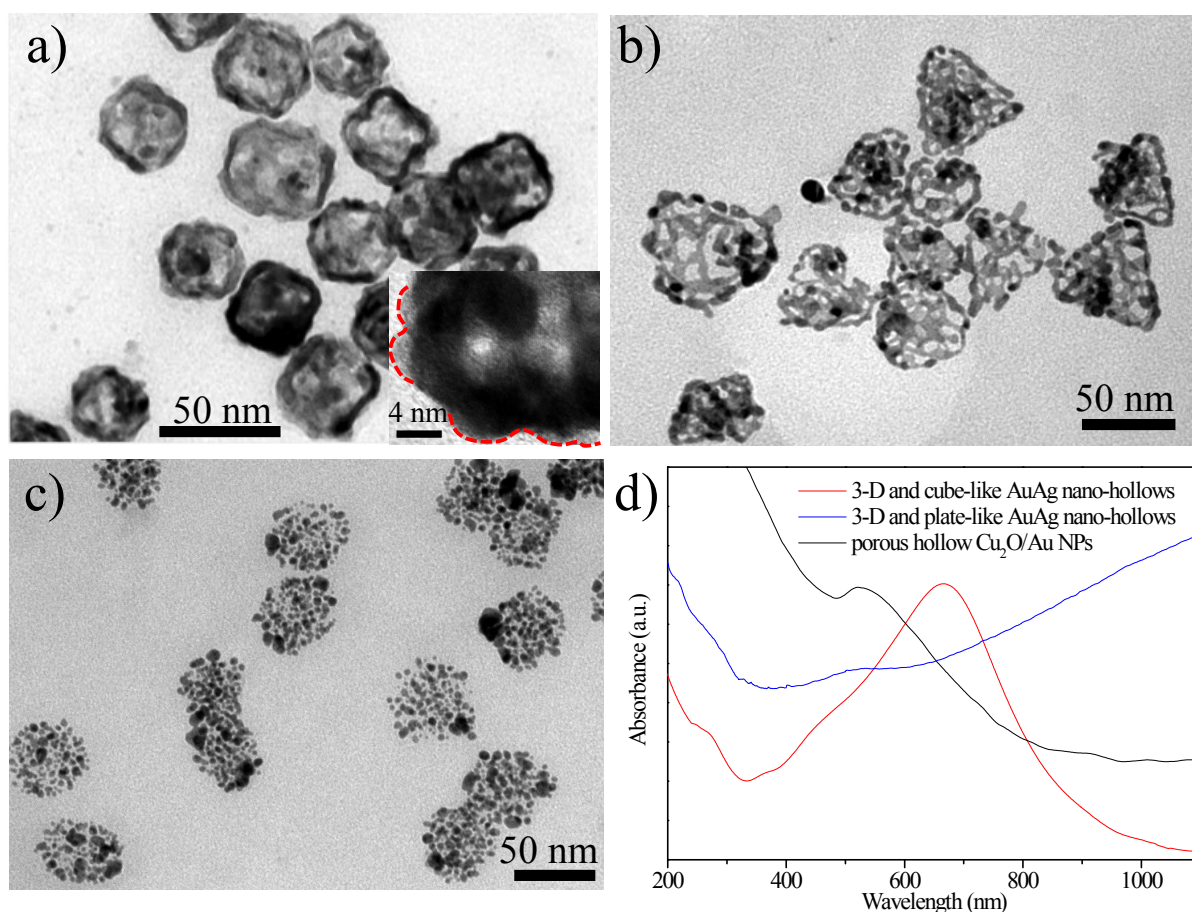


Figure S12. TEM images of the resulting hollow nanoparticles using PVP/PSMA-protected a) Ag nanocubes, b) Ag nanoplates, and c) Cu₂O nano-polyhedrons templates after reacting with 4 mL HAuCl₄ solution (0.04 mM) and 0.2 mL HNO₄ solution (0.22 M). d) UV-visible spectra of the solution samples from the nano-products a)-c).

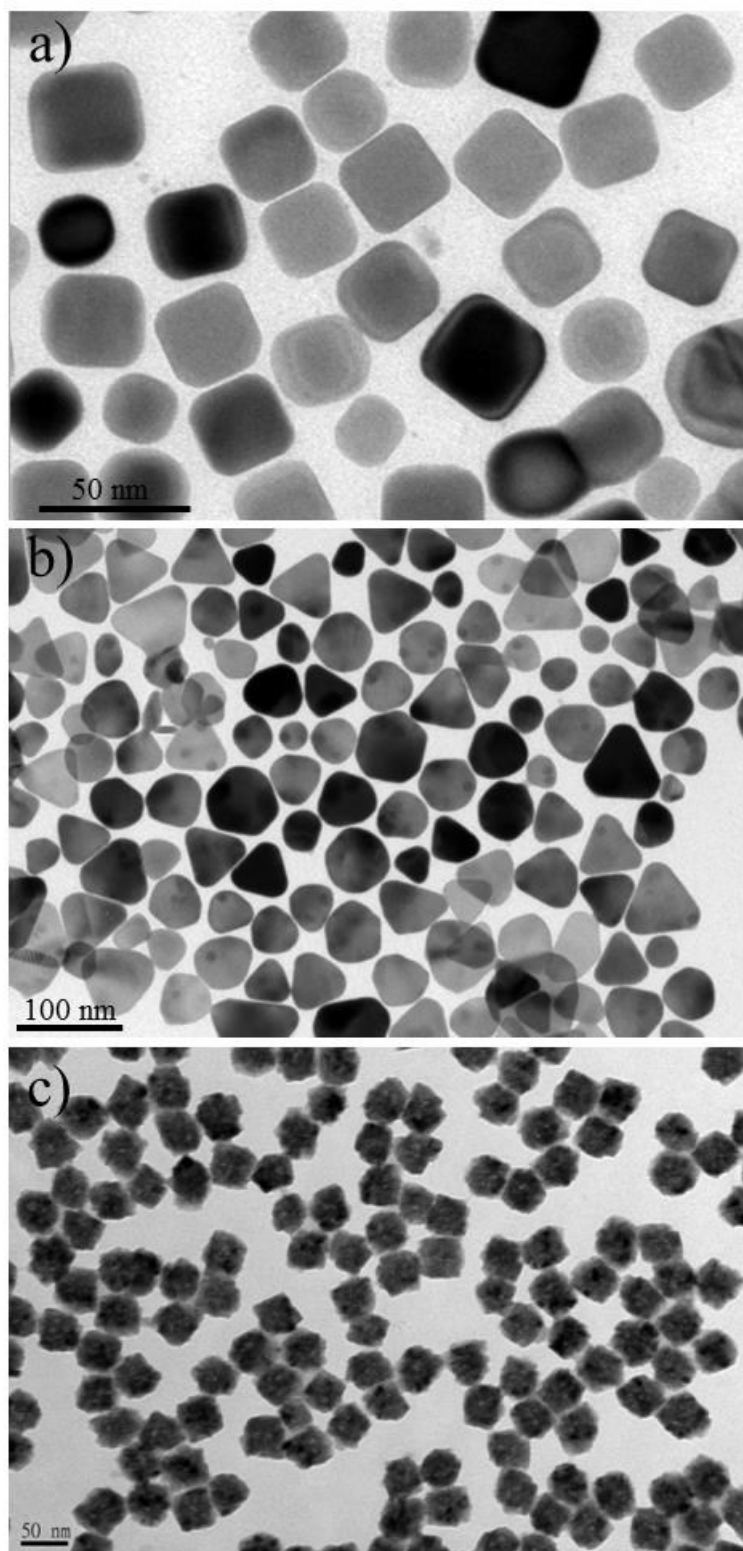


Figure S13. TEM images of a) Ag nanocubes, b) Ag nanoplates, and c) Cu₂O nanopolyhedrons.

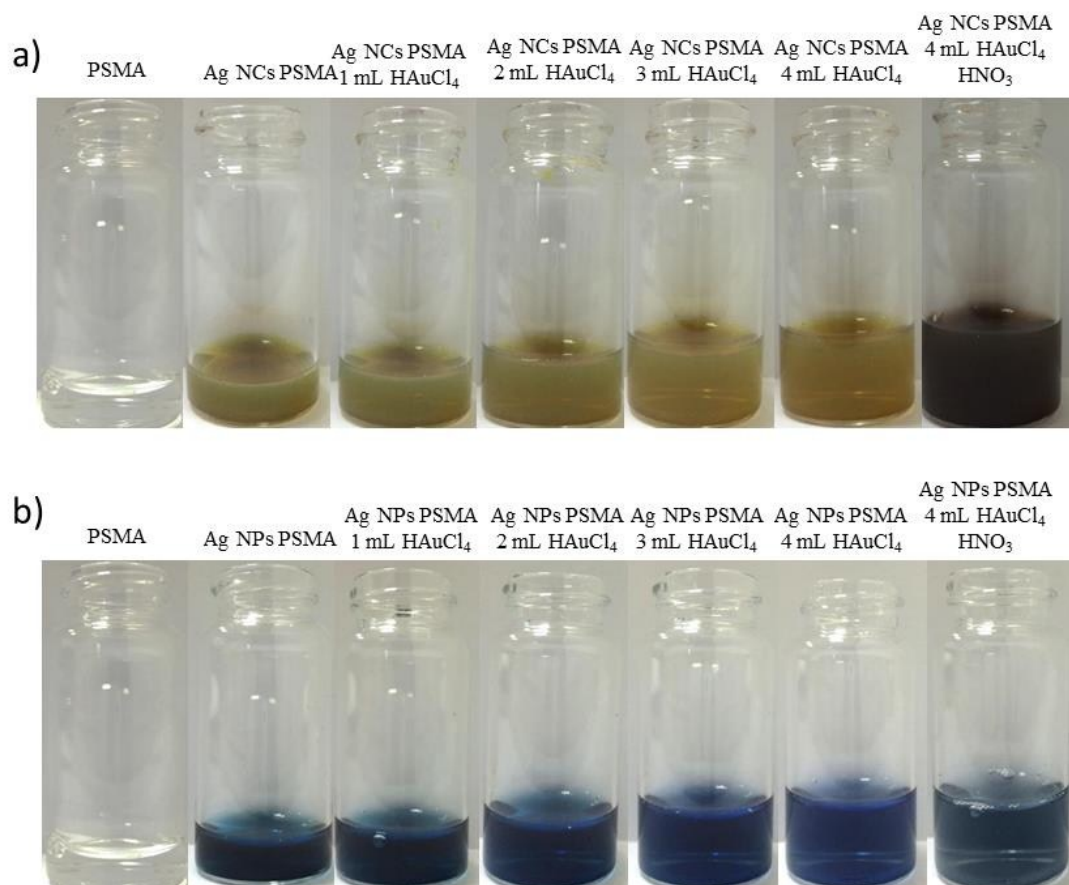


Figure S14. Images obtained while monitoring the color change of the a) PVP/PSMA-protected Ag nanocubes (NCs) and b) PSMA/PVP-protected Ag nanoplates (NPs) after the addition of H_{AuCl}₄ and HNO₃ solutions.

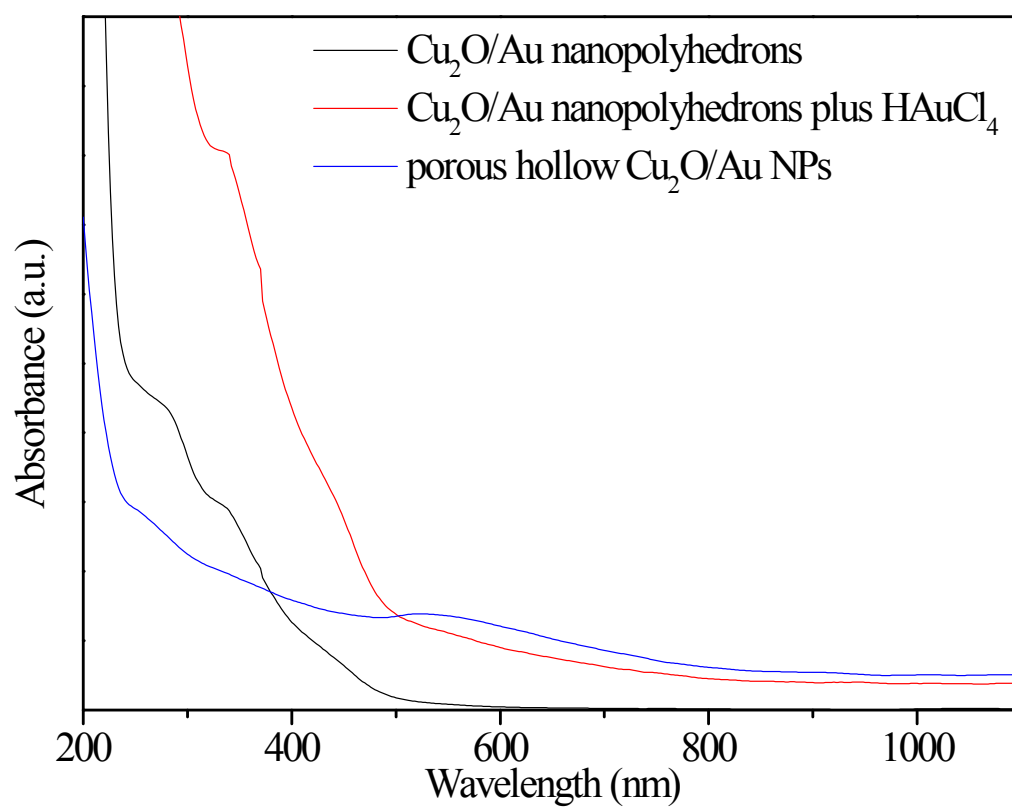


Figure S15. UV-visible spectra recorded the reactions of Cu₂O nanopolyhedron solution (black curve) with HAuCl₄ solution (red curve) and then added HNO₃ solution (blue curve) to prepare porous hollow Cu₂O NPs.

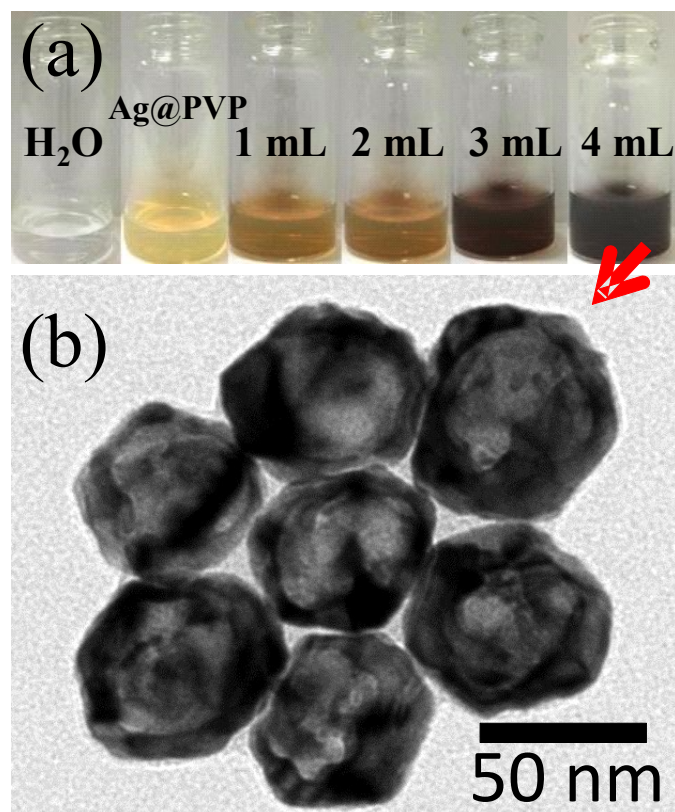


Figure S16. a) Images obtained while monitoring the color change of the PVP-protected Ag nanoparticles after the addition of the H₂AuCl₄ solution. b) The corresponding TEM images for the PVP-protected Ag nanoparticles after the addition of 4 mL of H₂AuCl₄ solution.

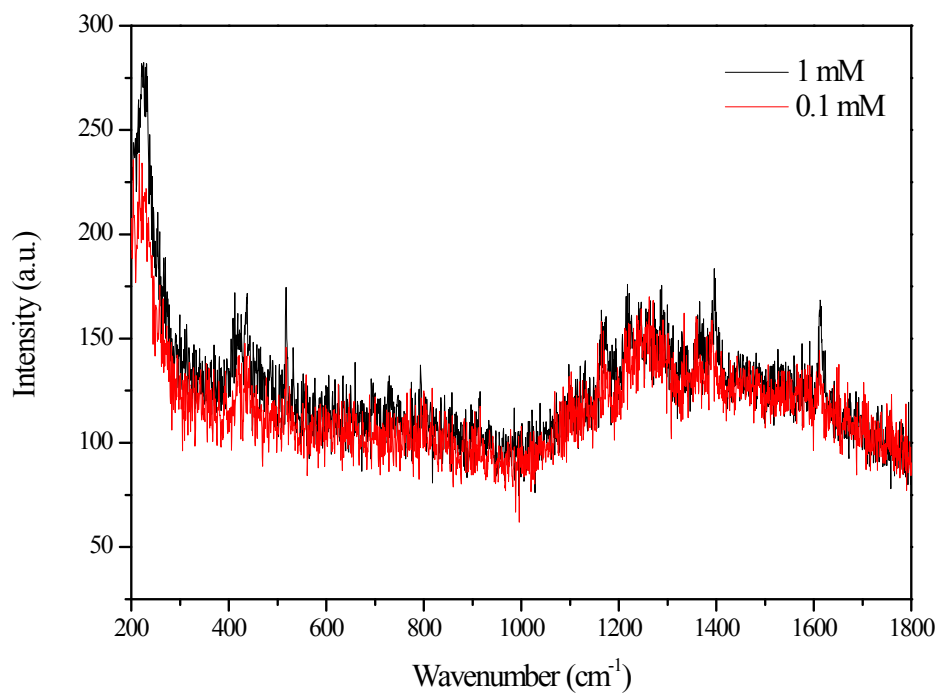


Figure S17. Raman spectra analysis of the mixture of PVP-protected AuAg nano-hollows with MG solution.

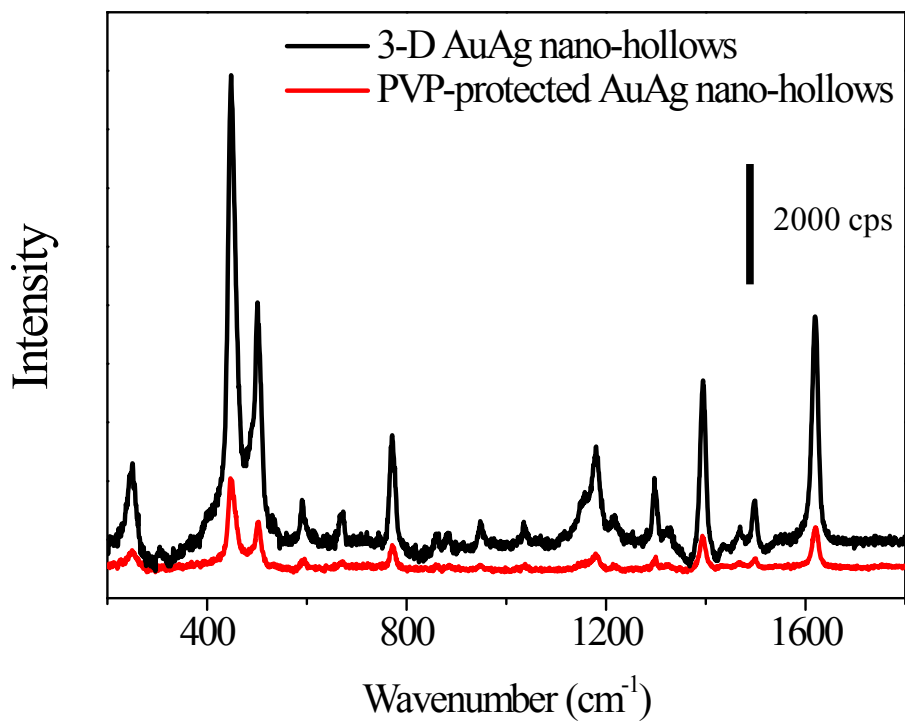


Figure S18. Surface-enhanced Raman spectroscopy of 0.1 mM MB solution mixed with 3-D AuAg nano-hollows (250 ppm) and PVP-protected AuAg nano-hollows (250 ppm).

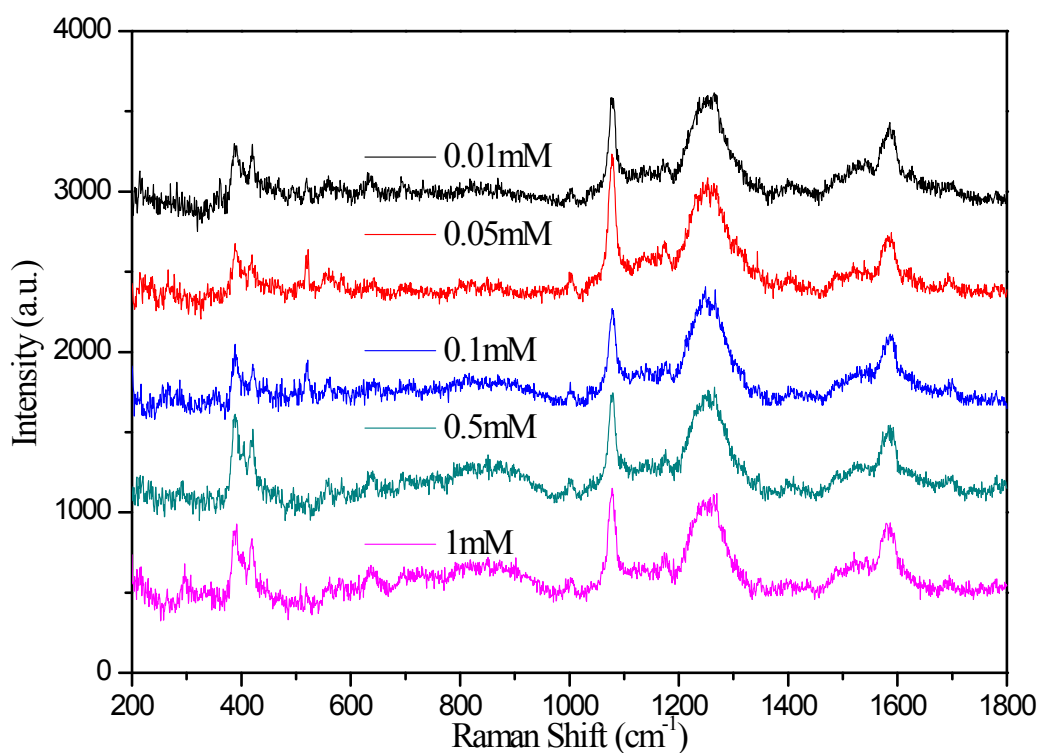


Figure S19. Raman spectra records of 10 μL of 3-D AuAg nano-hollows (25 ppm) including NaNO_2 with concentrations ranging from 1 mM to 1×10^{-2} mM in the existence of 23 mM HNO_3 and 0.27 mM H_2O_2 . Each data point was obtained during a 10 s acquisition

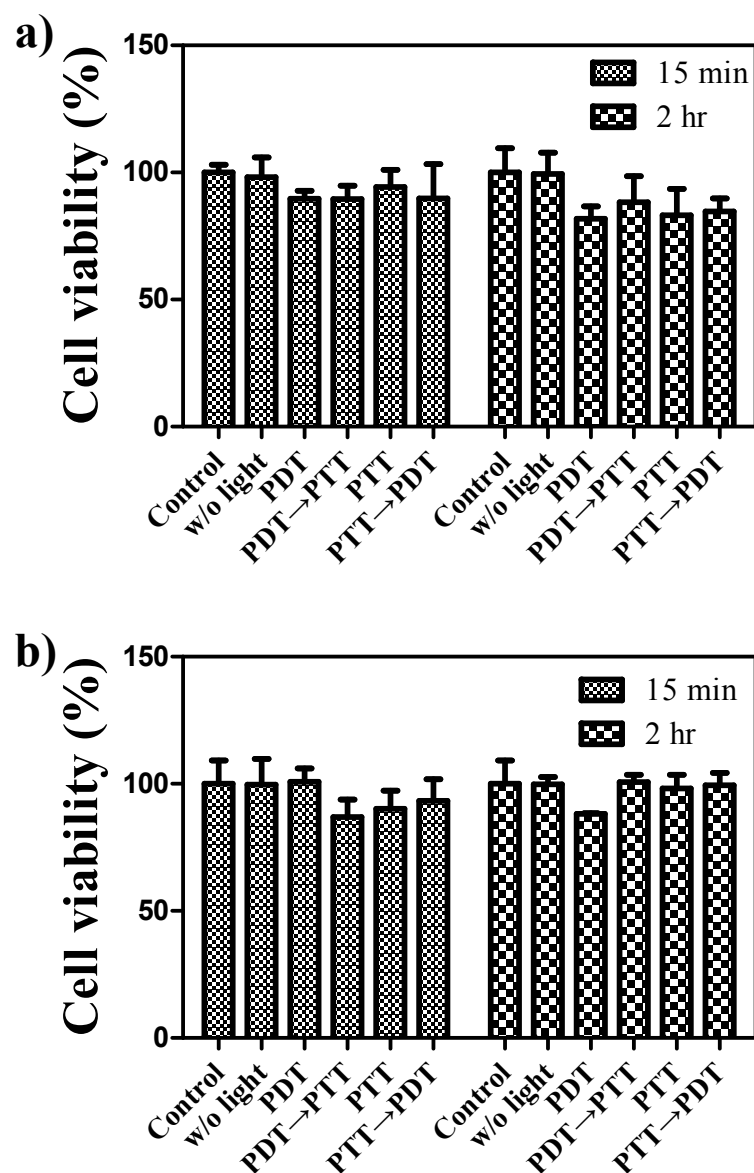


Figure S20. MTT assays for HeLa cells incubated with FA-AuAg@MB nano-hollows (PDT: 660 nm LED at 10 mW/cm² and 1 min and PTT: 808 nm laser at 380 mW/cm² and 1 min) and FA-free AuAg@MB nano-hollows (PDT: 660 nm LED at 10 mW/cm² and 4 min) and PTT: 808 nm laser at 380 mW/cm² and 3 min).